PROCEEDINGS OF SPIE

SPIEDigitalLibrary.org/conference-proceedings-of-spie

Mauna Kea Spectrographic Explorer (MSE): a conceptual design for multi-object high resolution spectrograph

Kai Zhang, Yongtian Zhu, Zhongwen Hu

Kai Zhang, Yongtian Zhu, Zhongwen Hu, "Mauna Kea Spectrographic Explorer (MSE): a conceptual design for multi-object high resolution spectrograph," Proc. SPIE 9908, Ground-based and Airborne Instrumentation for Astronomy VI, 99081P (9 August 2016); doi: 10.1117/12.2231935

Event: SPIE Astronomical Telescopes + Instrumentation, 2016, Edinburgh, United Kingdom

Mauna Kea Spectrographic Explorer (MSE): A Conceptual Design for Multi-object High Resolution Spectrograph

Kai Zhang*[a, b], Yongtian Zhu[a, b], Zhongwen Hu[a, b]
a. National Astronomical Observatories / Nanjing Institute of Astronomical Optics & Technology, Chinese Academy of Sciences, Nanjing 210042, China;
b. Key Laboratory of Astronomical Optics & Technology, Nanjing Institute of Astronomical Optics & Technology, Chinese Academy of Sciences, Nanjing 210042, China

ABSTRACT

The Maunakea Spectroscopic Explorer (MSE) project will transform the CFHT 3.6m optical telescope into a 10m class dedicated multi-object spectroscopic facility, with an ability to simultaneously measure thousands of objects with a spectral resolution range spanning 2,000 to 40,000. MSE will develop two spectrographic facilities to meet the science requirements. These are respectively, the Low/Medium Resolution spectrographs (LMRS) and High Resolution spectrographs (HRS). Multi-object high resolution spectrographs with total of 1,156 fibers is a big challenge, one that has never been attempted for a 10m class telescope. To date, most spectral survey facilities work in single order low/medium resolution mode, and only a few Wide Field Spectrographs (WFS) provide a cross-dispersion high resolution mode with a limited number of orders. Nanjing Institute of Astronomical Optics and Technology (NIAOT) propose a conceptual design with the use of novel image slicer arrays and single order immersed Volume Phase Holographic (VPH) grating for the MSE multi-object high resolution spectrographs. The conceptual scheme contains six identical fiber-link spectrographs, each of which simultaneously covers three restricted bands (λ/30, λ/30, λ/15) in the optical regime, with spectral resolution of 40,000 in Blue/Visible bands (400nm / 490nm) and 20,000 in Red band (650nm). The details of the design is presented in this paper.

Keywords: Maunakea Spectroscopic Explorer, Multi-object Spectrograph, High Resolution Spectrograph, Image Slicer Arrays, Immersed VPH grating

1. INTRODUCTION

The Maunakea Spectroscopic Explorer is an 11.25m aperture observatory with a 1.5 square degree field of view that will be fully dedicated to multi-object spectroscopy[1, 2]. 3,200 or more fibers will feed spectrographs operating at low (R ~ 2,000 – 3,500) and moderate (R ~ 6,000) spectral resolution, and approximately 1,156 fibers will feed spectrographs operating at high (R ~ 40,000) resolution. At low resolution, the entire optical window from 360nm – 950nm and the near infrared J and H bands will be accessible, and at moderate and high resolutions windows with the optical range will be accessible. The entire system is optimized for high throughput, high signal-to-noise observations of the faintest sources in the Universe with high quality calibration and stability being ensured through the dedicated operational mode of the observatory. The discovery efficiency of MSE is an order of magnitude higher than any other spectroscopic capability currently realized or in development.

* kzhang@niaot.ac.cn, phone: +86-25-8548-2316, www.niaot.ac.cn

Ground-based and Airborne Instrumentation for Astronomy VI, edited by Christopher J. Evans, Luc Simard, Hideki Takami
Proc. of SPIE Vol. 9908, 99081P · © 2016 SPIE · CCC code: 0277-786X/16/$18 · doi: 10.1117/12.2231935

A unique and scientifically powerful aspect of MSE is that it can obtain spectra for ~1,000 objects simultaneously at R=40,000. This enables detailed study of weak spectral lines in crowded regions, which is essential to probe various chemical species that provide key insights into the evolution of the Galaxy and the formation of the elements. For example, MSE at high resolution will have unmatched capability for "chemical tagging" experiments, that uses stellar chemistry to the building blocks of the Galaxy. The ESA space satellite Gaia[3] is dedicated to probing the properties of all stars brighter than G=20 magnitudes, and here MSE will be the ultimate Gaia follow-up facility. In particular, MSE will decompose the outer regions of the Galaxy – where dynamical times are long and whose chemistry is inaccessible from 4-m class facilities – into its constituent star formation events by accessing a range of chemical tracers that sample a large number of nucleosynthetic pathways. In so doing, MSE will provide a high resolution, homogenous sampling of the metallicity distribution function of the Galaxy.

PLATO[4], like Gaia, is another ESA mission, which is being developed in order to monitor a large number of bright stars to search for planets. MSE will provide spectroscopic characterization at high resolution and high signal to noise ratio of the faint end of the PLATO target distribution (g∼16), to allow for statistical analysis of the properties of planet-hosting stars as a function of stellar and chemical parameters. With high velocity accuracy and stability, MSE time domain spectroscopic programs will allow for highly complete, statistical studies of the prevalence of stellar multiplicity into the regime of hot Jupiters for this and other samples and also directly measure binary fractions away from the Solar Neighbourhood. A menagerie of rare stellar types will be identified in MSE multi-epoch spectroscopic datasets that will allow for population studies of in-situ stars across all components of the Galaxy, at all galactocentric radii and at all metallicities. For all of this science, the high resolution capability of MSE is essential.

To promote these scientific research, the MSE High Resolution Spectrograph (HRS) faces as high requirement as the specification list in Table (1). Its conceptual design is described on Section 2; the method adopted to get the required resolution is discussion on Section 3; the optics of spectrograph is introduced on Section 4; a final summary is given on Section 5.

Table 1. The general specification of MSE HRS

Parameters	Requirement	Conceptual Design
The number of objects	1,156 (386 each)	1,200 (200 objects each)
The number of spectrographs	3	6
Fiber	0.9" – 1.2"	1.0", goal: 1.2"
Spectral resolution	R 40,000 in Blue / Visible, R 20,000 in Red	Meet
Spectral coverage	λ/30 in R 40,000 mode, λ/15 in R 20,000 mode	401.8 – 415.3 nm (B), 481.8 – 498.1 nm (V) , 629.0 – 672.0 nm (R)

2. CONCEPTUAL DESIGN

More and more astronomical optical facilities are involved in the survey observation (SDSS, LAMOST, VISTA, LSST). Although several spectroscopic projects around the world are in advanced stages of development, all of these take the form of either instruments for 4-m and 8-m class telescopes, or 4-m class spectroscopic facilities, see in Table (2)[2,5].

Only AAT/HERMES[6] stands out as the instrument that is geared exclusively towards high resolution (R28,000 / 45,000). Obviously, multi-object high resolution spectrographs with total of 1,156 fibers is a big challenge, one that has never been attempted for a 10m class telescope (MSE). Recently, high multiplexing has been achieved by replicating many spectrograph units, as in MUSE[7] and VIRUS[8], two integral field spectrographs. So it must be the trend for multi-object high-resolution spectrographs on large / extreme large telescope.

Table 2. Existing and planned multi-object spectroscopic capabilities (>300 objects)[2,5]

Project	Tel. Aperture (m)	FOV (Sq deg)	Fibers	Resolution	Grating type	Status
SDSS III/APOGEE	2.5	1.54	300	27,000 – 31,000	VPH	Existing
SDSS III / BOSS	2.5	7.07	1,000	1,500 – 2,500	VPH	Existing
Mayell/BigBOSS	3.8	7.07	5,000	5,000	VPH	Developing
AAT/AAOmega	3.9	3.14	392	1,300 – 8,000	VPH	Existing
AAT/HERMES	3.9	3.14	392	28,000 / 45,000	VPH	Existing
LAMOST/LRS	4.0	19.6	4,000	LR 1,800 / MR 7,500	VPH	Existing
VISTA/4MOST	4.0	4.0	MR 1624 HR 812	MR 4,000-7,800 HR 18,500	VPH	Developing
WHT/WEAVE	4.2	3.14	1,000	MR 5,000 / HR 20,000	VPH	Developing
MMT/HECTOSPEC	6.5	0.79	300	1,000	Reflective ruled	Existing
MMT/HECTOCHELLE	6.5	0.79	240	40,000	Echelle	Existing
SUBARU/PFS	8.2	1.78	2,400	2,000 – 5,000	VPH	Developing
VLT/MOONS	8.2	0.14	1,000	MR 4,000 – 6,000 HR 20,000	VPH	Developing
HET/VIRUS	9.2	19.6	33,600	700	VPH	Developing
MSE/LMRS	10.0	1.5	3,468	LR 2,500 – 3,000 MR 5,000 – 7,000	VPH	Planned
MSE/HRS	10.0	1.5	1,156	Blue 40,000 / Red 20,000	VPH	Planned

To date, most spectral survey facilities work in single order low/medium resolution mode, and only a few Wide Field Spectrographs (WFS) provide a cross-dispersion high resolution mode with a limited number of orders, see in Table (2). For MSE HRS, the required wavelength coverage in the resolution mode of 40,000 is about λ/30, equivalent to 14nm at 410nm. It needs 3 or 4 orders of spectra when the echelle grating is in charge of dispersion. As a result, the number of spectrographs increases at least 3 times more than the single order dispersion. The instrumental scale and cost would be unacceptable. So the conceptual design presented here is based on single order dispersion with some frontier technology.

$$R \times \varphi = 2 \times n \times \tan(\theta_B) \times \frac{D_C}{D_T} \times FRD \times 206265'' \quad (1)$$

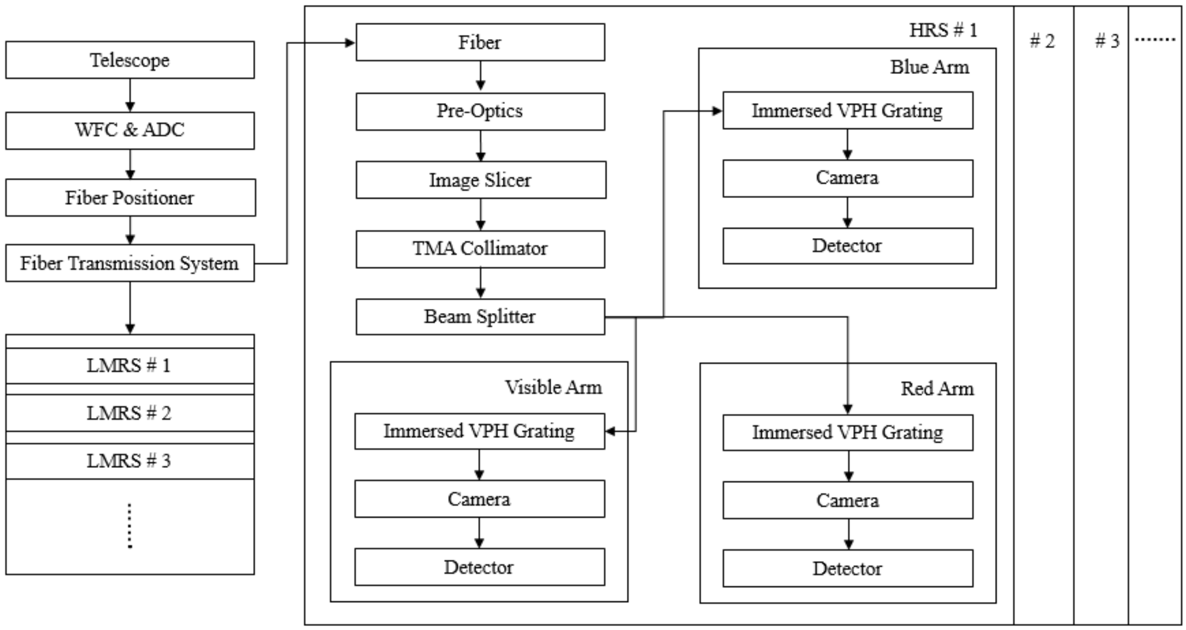

Figure 1. Working flow of MSE HRS

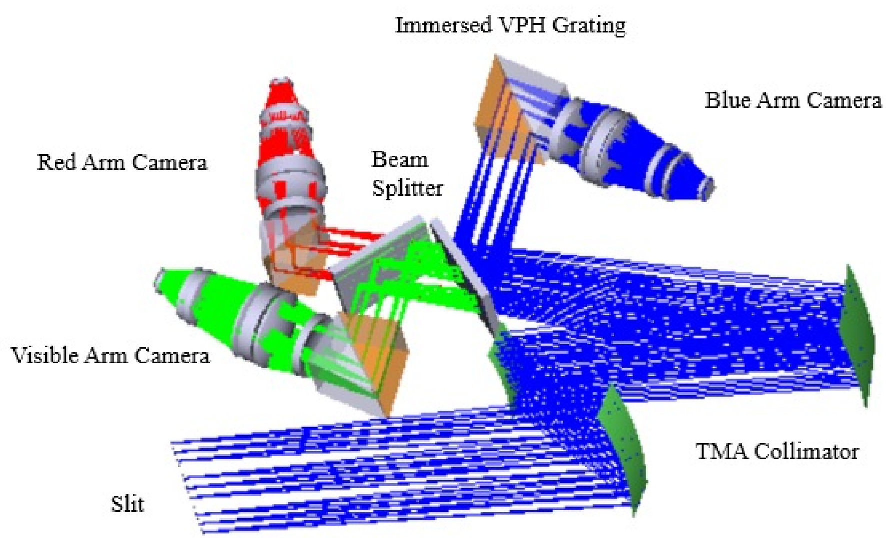

Figure 2. Optical design for MSE HRS without pre-optics and image slicer array

Through the basic calculation of dispersion power, see the equation (1), there're three elements to increase the resolution, respectively slit width on sky (φ), beam aperture (Dc), grating parameters (Blaze or Bragg angle (θ_B), the medium index (n)). Normally, high dispersion grating is the first direct way to enhance the instrumental dispersion power ($R \times \varphi$), but the VPH grating with an oversize Bragg angle cause great manufacture problem and efficiency loss, e. g. the VPH grating with Bragg angle of 68 degree in AAT/HERMES is bigger than 500 x 210 mm when the beam aperture is 190 mm in diameter[6]. Besides of the grating, slit width on sky (φ) and beam aperture (Dc) are also the popular way applied on most of the known spectrographs. Slit width on sky (φ) can be reduced by image slicer, and beam aperture (Dc) can be enlarged by pupil slicer as well. The result produced by both the methods is similar, but they has their own advantage and disadvantage. The former increases the spectral resolution (R) but not dispersion power. The number of spectrographs has to be increased by the slicing number. The latter increases both of the spectral resolution and dispersion power ($R \times \varphi$), but the number of spectrographs increased more rapidly than the way with image slicer[5].

With the consideration to take use of the existing technology in Maximum, the conceptual design adopts both of image slicer and immersed VPH grating to achieve the required resolution and control the instrumental cost and scale. Six identical spectrographs can fully cover the total 1,156 objects. Figure (1) shows the working flow of MSE high resolution spectrographs, and Figure (2) shows the current optical design of single spectrograph.

3. SPECTRAL RESOLUTION

Fiber

Depend on the strong light-gather power, MSE focuses the faint light from the universe on the fiber through the Wave Front Corrector (WFC) in the Top-End system. The input focal ratio of 2.0 is so fast as to keep 95% of the light within a focal ratio 5% larger than the F/2.0 illuminating the fibers. Each fiber held by a fiber positioner scans in a circular range, which has some overlapped zone with the adjacent units. ~ 3,200 fibers go down to the instrument platform (Nasmyth) and select 1,156 fibers to the Coude room for HRS through the optical switchers.

Bigger core diameter enable to gather more light from faint objects in the non-ideal site seeing, or improve the observation efficiency through reduce the exposure time. On the other hands, the core diameter indirectly make influence to the instrument design as well. The spectral resolution reduces with increasing of core diameter when the instrumental dispersion power is constant. In contrary, the parametric product, $\mathrm{n} \times \tan\theta_B \times D_c$, changes with the different core diameter when substitutes the known parameters into the equation (1), see in Table (4). The acceptable range of 0.9" – 1.2" makes the difference of up to 25% in the product.

It's well known that choice is always the result of a compromise between science and technology. The conceptual design chooses the conventional value of 1.0", which is chosen by most of the astronomical spectrographs on the similar site condition, and the goal is 1.2" in future. The total fibers is evenly distributed to six spectrographs, about 200 fibers each. On the entrance of single spectrograph, the fibers arrange in a line along the slit direction.

Image Slicer Array

Image slicer is widely applied for single object high resolution spectrographs, especially Bowen-Walraven type[9] (Subaru/HDS, VLT/UVES and Mercator/HERMES). The rare application in multi-object high resolution spectrograph is because of its complexity and the spatial limitation. A kind of transmission image slicer[10] with compact symmetric structure is possibly the key to open the door for this application. Compared with the Bowen-Walraven type, their advantage and disadvantage are impressive and targeted, see in Table (3). To Bowen-Walraven type, complexity and image defocus are unacceptable disadvantage for multi-object spectrograph. To transmission type, the disadvantage in chromatic aberration and virtual image are not good but acceptable. With the symmetric characteristics, transmission image slicer provides friendly interface for modularization and assembly.

Differ from single-object spectrograph, the slicing number determines the detector area to cover all of spectra when camera's focal ratio is fixed, however, the field of view of camera is actually limited by manufacture capability and throughput. Conceptual design chooses 2-slicing image slicer array in order to adopt compact detector with only a single CCD chip. The field of view of camera doesn't exceed 17 degree in diameter.

Table 3. Technical comparison on image slicer

	Bowen-Walraven type	Transmission type
Cons	Complexity, Spatial limitation, Defocus	Virtual slit, Chromatic aberration
Pros	High throughput, Real slit	Confocus, Modularization

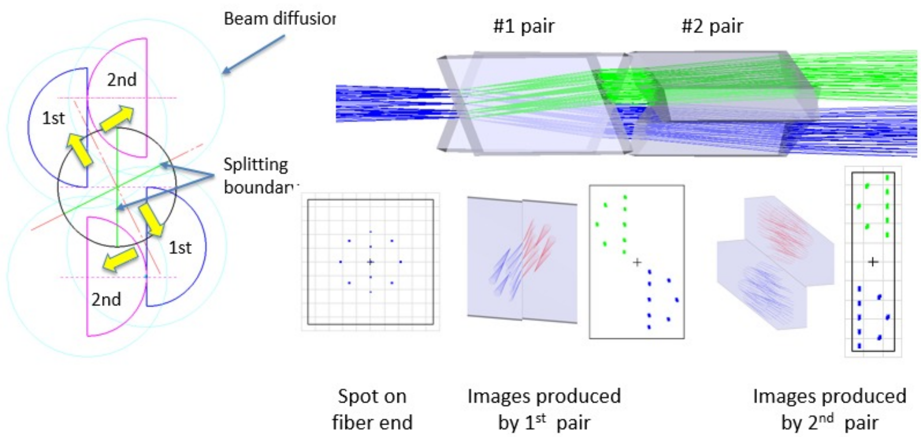

Figure 4. Working principle of the transmission image slicer

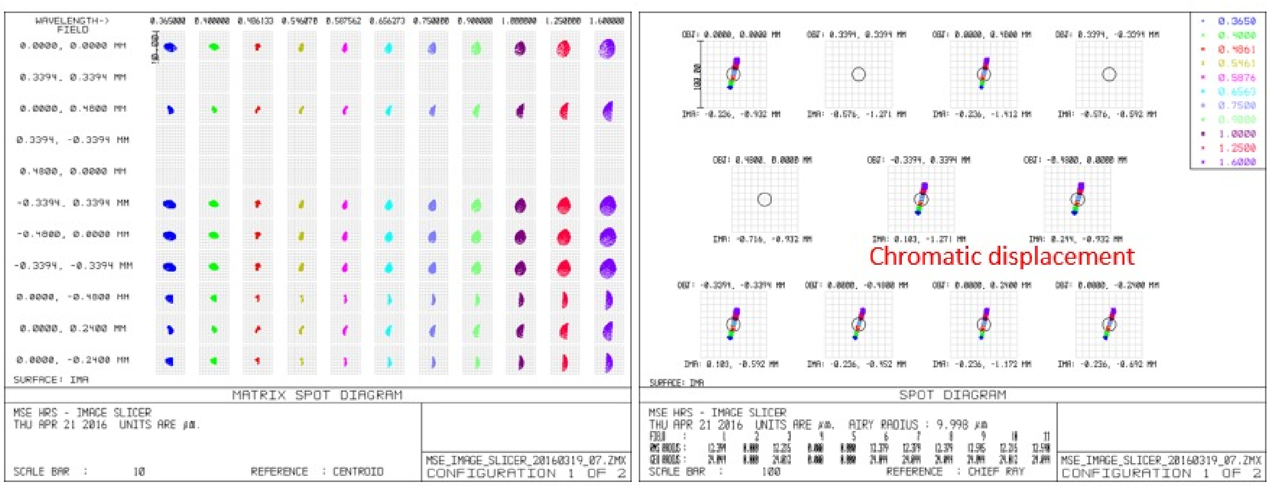

Figure 5. Image quality of image slicer

Theoretically, a single pair of 2-slicing image slicer is composed of 2 identical plates with the specified tilt. They are combined together with the opposite surfaces along the slicing direction. The image is splitted by the glass edge on the combined surface. But sliced images have a small interval in dispersion direction when only a pair of image slicer is applied. The conceptual design tries two pairs of image slicer in order to arrange the sliced images are in a common line. The image motion made by two pairs of image slicer are orthogonal and equivalent in the radial plane. The second pair double the motion along the slit, and compensate the motion made by the first one in the orthogonal direction, see in Figure (4). On image quality, the main degradation comes from chromatic aberration due to the medium index, see in Figure (5).

Immersed VPH Grating

Optical material is always the important element to consider even if the reflective optics. Most of the current multi-object spectrographs on the 4 – 8m class telescopes control the aperture of the collimated beam to be not bigger than 300 mm in diameter, see in Table (2). And it's smaller than 200 mm in diameter when the dioptric camera is used. Due to this moderate aperture range and image slicer array, the spectrograph have to select the oversize VPH grating with size of more than 550 mm and Bragg angle of more than 60 degree in air, see in Table (4a). Even if the similar grating is successfully applied in AAT/HERMES, Bragg angle of more than 60 degree in air and high groove density are not regular to a single order dispersion grating. In order to reduce the aperture and Bragg angle, the immersed VPH grating is possibly more suitable for MSE HRS. With the comparison in Table (4), it's shown that high index medium help to reduce the requirement to Bragg angle and grating size. But it has to be admitted that the groove density increases with the refractive index. Figure (6) shows the aperture decreases more rapidly than the increasing of groove density. It supports the choice of immersed VPH grating in conceptual design.

Table 4 (a). Relationship among the dispersion power, fiber and beam aperture (Air, n = 1)

$n \times \tan\theta_B \times D_c$	Fiber \ Dc	150mm	200mm	250mm	300mm	350mm
459.3	0.9"	72deg	66deg	62deg	57deg	53deg
510.3	1.0"	74deg	69deg	64deg	60deg	56deg
561.4	1.1"	75deg	71deg	66deg	62deg	58deg
612.4	1.2"	76deg	72deg	68deg	64deg	60deg

Table 4 (b). Relationship among the dispersion power, fiber and beam aperture (Fused Silica, n = 1.47)

$n \times \tan\theta_B \times D_c$	Fiber \ Dc	150mm	200mm	250mm	300mm	350mm
459.3	0.9"	64deg	57deg	51deg	46deg	42deg
510.3	1.0"	67deg	60deg	54deg	49deg	45deg
561.4	1.1"	69deg	62deg	57deg	52deg	48deg
612.4	1.2"	70deg	64deg	59deg	54deg	50deg

Table 4 (c). Relationship among the dispersion power, fiber and beam aperture (PBM2Y, n = 1.65)

$n \times \tan\theta_B \times D_c$	Fiber \ Dc	150mm	200mm	250mm	300mm	350mm
459.3	0.9"	62deg	54deg	48deg	43deg	39deg

510.3	1.0”	64deg	57deg	51deg	46deg	41deg
561.4	1.1”	66deg	60deg	54deg	49deg	44deg
612.4	1.2”	68deg	62deg	56deg	51deg	47deg

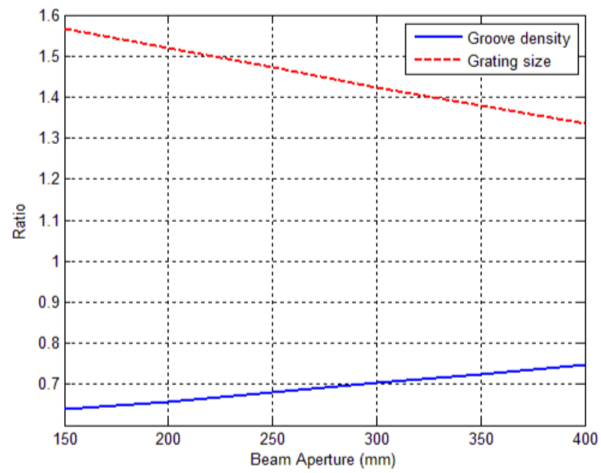

Figure 6. Comparison between VPH and immersed VPH gratings

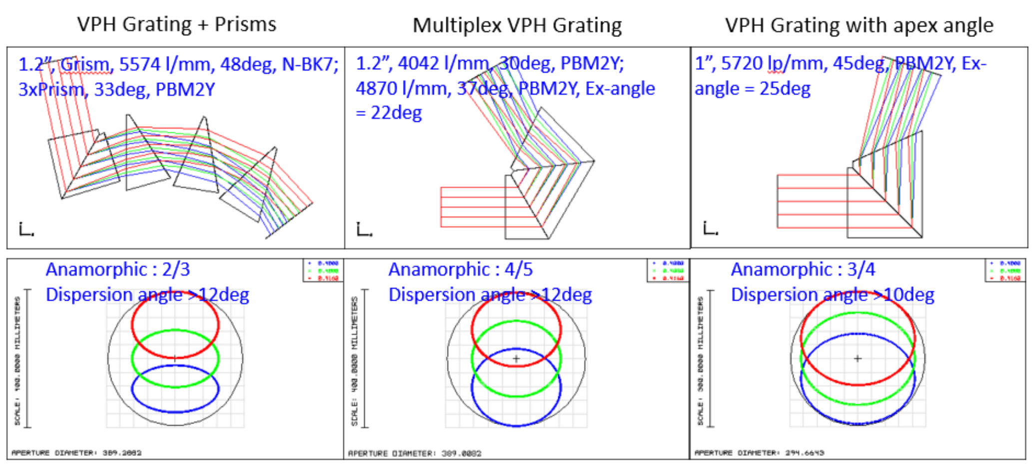

Figure 8. Study on grating design (Top: Three grating design; Bottom: Anamorphic aperture)

As well as we know, the VPH grating has unparalleled advantage in high groove density of 600 – 5,000 lp/mm, however, the manufacture face challenge when the groove density goes up to 6,000 lp/mm or higher. The collimated beam of 250 mm in diameter is chosen in according to trade-off study. The groove density is about 6,410 lp/mm at 410 nm, and the grating is immersed in a pair of PBM2Y prism with aperture of 420 x 250 mm. Obviously, this is still not the best result for MSE HRS. Another study based on the immersed VPH grating is initiated to further reduce the groove density. Some different kinds of dispersers are involved, respectively multi-VPH grating, the combo with grating and prism and so on, see in Figure (7). Extra prism relieve the grating’s pressure and reduce the dispersion difference at short and long wavelength. Finally, the immersed grating with extra apex angle of 25 degree on the last surface is chosen for the present conceptual design. It respectively reduces the groove density down to 5,720 lp/mm at 410nm, and the grating aperture down to 360 x 250 mm, the other gratings are list in Table (5).

Table 5. Specification of immersed VPH gratings

Parameters	Blue arm	Visible arm	Red arm
Resolution mode	40,000	40,000	20,000
Material of prism	PBM2Y	PBM2Y	PBM2Y
Bragg angle	45 degree	47 degree	35 degree
Groove density	5,720 lp/mm	4,925 lp/mm	2,850 lp/mm
Extra apex angle	25 degree	25 degree	0 degree

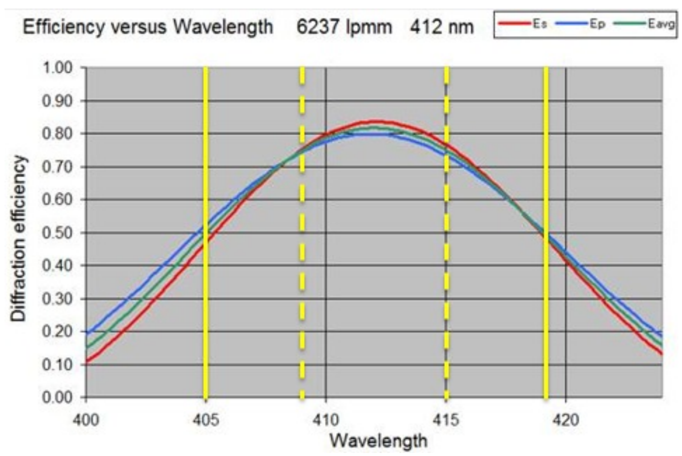

Figure 9. Variation of diffraction efficiency with wavelength (Bragg angle = 58 degree, S-BSL7)

The third factor in the grating selection is throughput over the wavelength range. For the immersed grating, diffraction efficiency decreases rapidly with wavelength due to high groove density and big Bragg angle. Fortunately, narrow wavelength coverage gives chance to keep diffraction efficiency higher than 50% over the whole spectral range, see in Figure (9). In addition, the off-axis fibers possibly reduce the diffraction efficiency due to 'out of the plane' angle.

In a word, 1" fiber, 2-slicing image slicer array, 250mm beam aperture and immersed grating with extra apex angle are all the means adopted to achieve the required resolution in conceptual design.

4. OPTICS

4.1 Pre-Optics

Pre-optics slows the fast beam from fibers down to be F/20, and focuses on the entrance of image slicer. Maximum aperture of ~ 4 mm in diameter exceed the adjacent spacing of sliced images so that an array of fold mirrors with different angles provide adequate space for every unit, see in Figure (10).

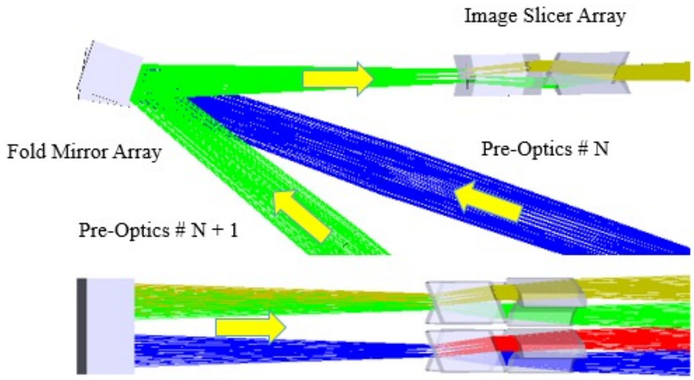

Figure 10. Pre-Optics (Top: local model in top view; Bottom: local model in side view)

4.2 TMA Collimator

The conceptual design chooses a Three Mirrors Anastigmatic (TMA) collimator, which covers a field of view of ±5.3 degree in slow focal ratio of F/20, see in Figure (2). Slow focal ratio makes 'out of the plane' angle so small that diffraction efficiency possibly reduces by ~ 5%. TMA optics also bring better wavefront quality on the grating than the conventional ones of Schmidt or Houghton design, see in Figure (11).

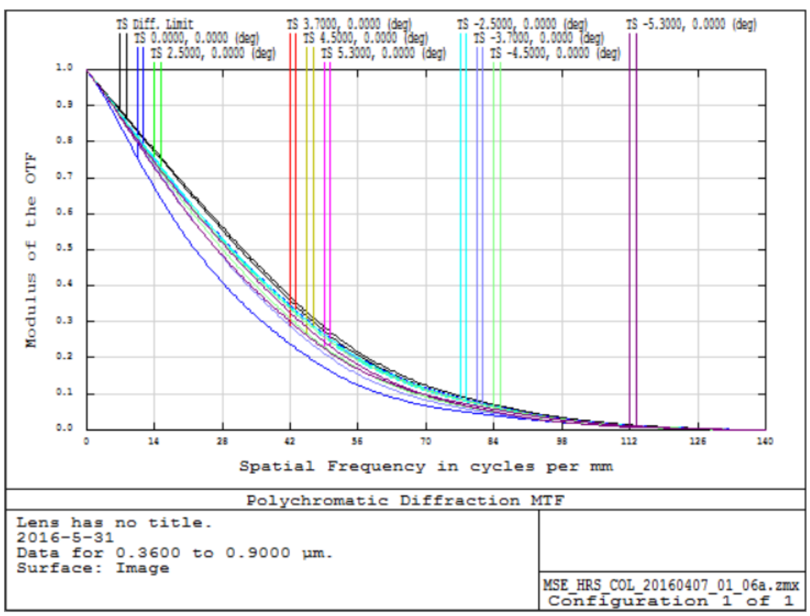

Figure 11. MTF of TMA Collimator

4.3 Beam Splitter

The beam splitters that define the wavelengths for the four channels are as follows: 401.8 – 415.3 nm (B), 481.8 – 498.1 nm (V) and 629.0 – 672.0 nm (R), see in Figure (2) and (12). The cutting off wavelength in 450 nm and 600 nm is produced by the dichroic coating. The dimensions of the Fused Silica substrates are 460 x 540 mm with a thickness of

50mm. The blue arm get the beam by the reflection on the first beam splitter. The red arm get the beam by transmission after the second beam splitter.

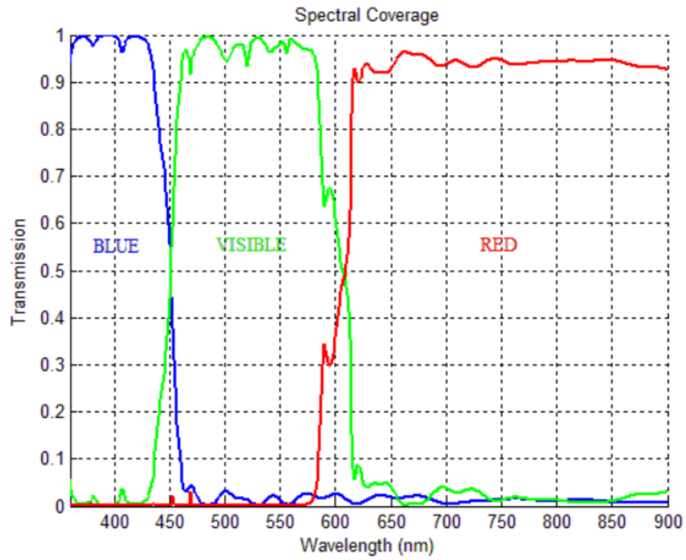

Figure 12. Spectral coverage given by dichroic coating (360 – 900 nm)

4.4 Camera

The cameras are fairly fast with a focal ratio of 1.8. Its field of view of 17 degree in diameter fully cover a single CCD chip with 9K x 9K @ 10 um, see in Figure (13). The largest elements are the second and third lenses with a diameter of 410mm. All of the optical surfaces are spherical but not the first surfaces of second and fifth lenses. The single CCD chip accommodates the spectra for 200 objects, see in Figure (14). The spectra separation is about 40 pixels, which accommodates two sliced images of 5 x 10 pixels each. Imaging performance meet the requirement as well, RMS diameter without image slicer is smaller than 0.2" at all wavelengths, see in Figure (15).

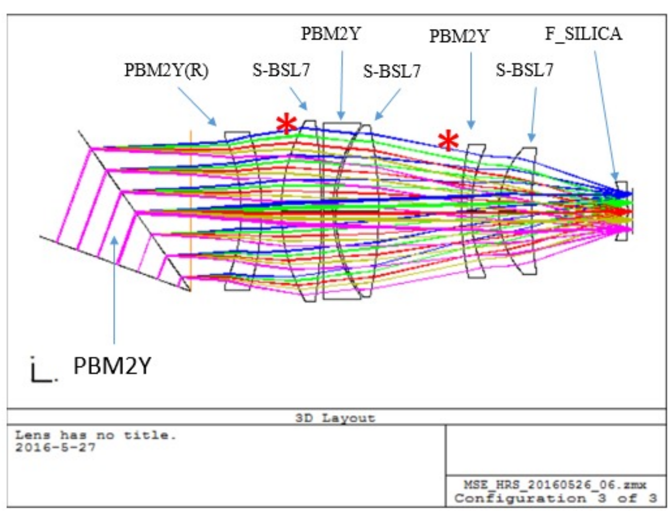

Figure 13. Optics for blue arm camera (The other cameras have similar optics)

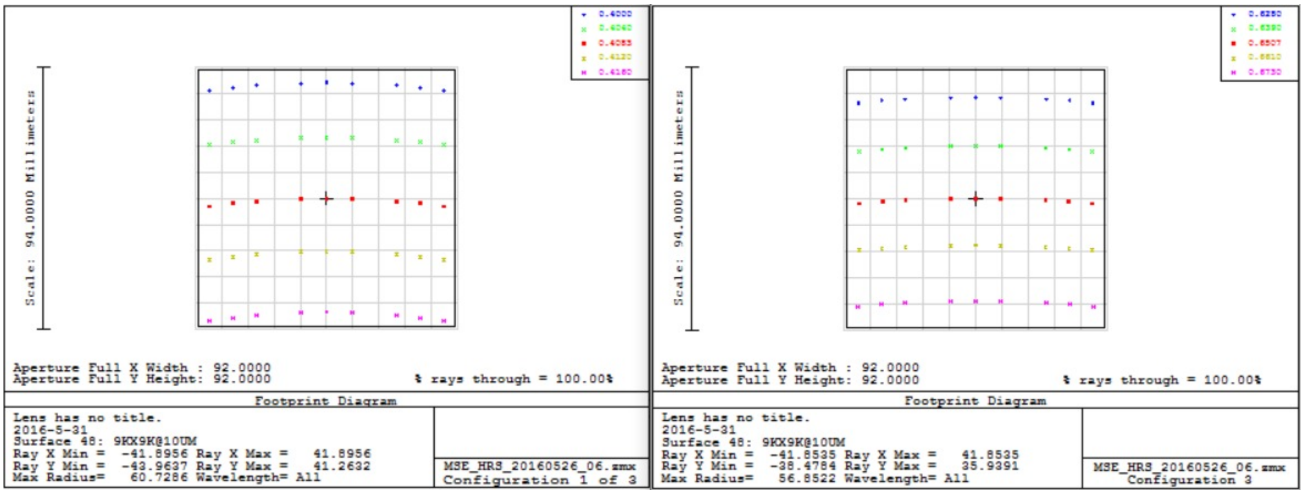

Figure 14. Spectra pattern on the detector (Left: Blue arm; Right: Red arm)

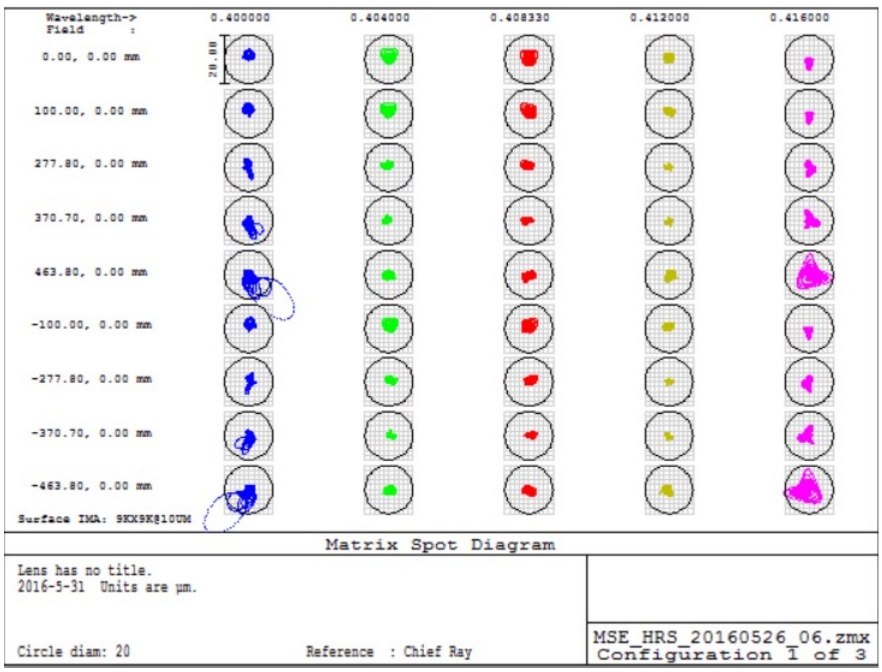

Figure 15. Spot matrix in blue arm (Circle: 0.2" on sky)

5. SUMMARY

The design with image slicer array and immersed VPH grating gives a feasible solution for MSE multi-object high resolution spectrographs, but not the best one. Demand of six identical spectrographs and oversize materials makes instrumental cost quite high. The grating performance in diffraction efficiency and polarization is in need of further analysis, the spectra deviation caused by the 'out of plane' angle is possibly solved out by curving the slit laterally. Due to image slicer, difficulty in data reduction shall be considered carefully as well. In a word, this design is good beginning for MSE HRS even if there's a lot of work to do.

6. ACKNOWLEDGEMENTS

This work is supported by the Nanjing Institute of astronomical Optics and Technology (NIAOT) and the MSE Project Office. The funding partly comes from the National Natural Science Foundation of China (NSFC) project (11503062), the Natural Science Foundation of Jiangsu province (BK20151065), the special funds for equipment renewal at astronomical observatory and major equipment operation, and the knowledge innovation engineering in young talents field, NIAOT. We give our sincere thanks to Rick Murowinski, Alan McConnachie, Kei Szeto, Nicolas Flagey (MSE project office), Derrick Salmon (Canada-France-Hawaii Telescope Corporation), Shan Mignot (Observatoire de Paris), and Will Saunders (Australian Astronomical Observatory). They generously gave much meaningful comment on the conceptual design. Also give thanks to the company, Wasatch Photonic, for the grating technology consulting.

REFERENCES

[1] D. A. Simons, D. Compton, P. Côté, A. McConnachie., et al., "Current status and future plans for the Maunakea Spectroscopic Explorer (MSE)," Proc. SPIE 9145, 91451501-91451511 (2014).

[2] Alan M., Rick M., Derrick S., Doug S., Patrick C., "The Maunakea Spectroscopic Explorer: the science-driven design rationale," Proc. SPIE 9145, 91451901-91451912 (2014).

[3] J.H.J. de Bruijne, "Science performance of Gaia, ESA's space-astrometry mission," Ap&SS 341(1), 31-41 (2012).

[4] C. Catala, "PLATO: PLAnetary Transits and Oscillations of stars," ExA 23(1), 329-356 (2009).

[5] P. Spanò, "MSE spectrograph optical design: a novel pupil slicing technique," Proc. SPIE 9147, 91474D01-91474D12 (2014).

[6] S. C. Barden., D. J. Jones, S. I. Barnes, et al., "HERMES: revisions in the design for a high-resolution multi-element spectrograph for the AAT," Proc. SPIE 7735, 77350901-77350919 (2010).

[7] G. J. Hill, H. Lee, B. L. Vattiat, et al., "VIRUS: a massively replicated 33k fiber integral field spectrograph for the upgraded Hobby-Eberly Telescope," Proc. SPIE 7735, 77350L01-773512 (2010).

[8] F. Henault, R. Bacon, C. Bonneville, et al., "MUSE: a second-generation integral-field spectrograph for the VLT," Proc. SPIE 4841, 1096-1107 (2003).

[9] Th. Walraven, J. H. Walraven, "Some features of the Leiden radial velocity instrument," Proc. AILT 175, (1972).

[10] G. Avila, C. Guirao, T. Baader, "High efficient inexpensive 2-slices image slicers," Proc. SPIE 8446, 84469M01-84469M06 (2012).

[11] P. Spanò, F. M. Zerbi, C. J. Norrie, C. R. Cunningham, et al., "Challenges in optics for Extremely Large Telescope instrumentation," Astron. Nachr. 327(7), 649–673 (2006).